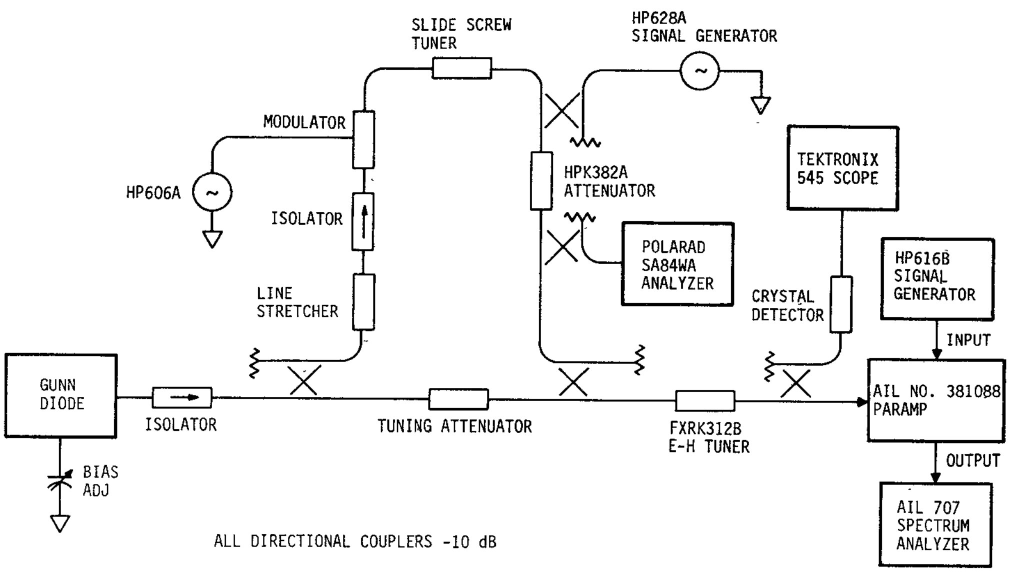

Fig. 2. Experimental arrangement.

ACKNOWLEDGMENT

The authors wish to thank J. F. Craib and J. A. DeGruyl for their helpful suggestions.

REFERENCES

[1] D. M. Clunie, K. R. Heath, C. A. Tearle, and J. C. Vokes, "IMPATT driven pumps for parametric amplifiers," *SERL Tech. J.* vol. 21, Paper 12, Oct. 1971.
[2] R. J. Wagner, W. W. Gray, and A. Luber, "The use of IMPATT generated power for parametric amplifier pumps," in *Proc. IEEE Int. Solid-State Circuit Conf.*, Feb. 1971, pp. 22–23.
[3] T. Smith, B. Smilowitz, G. Irvin, and R. Kaminsky, "IMPATT pump for low noise parametric amplifier," *IEEE Trans. Microwave Theory Tech.*, to be published.
[4] P. A. Levine, H. C. Huang, and H. Johnson, "IMPATTs shoot for Gunn noise levels," *Microwaves*, pp. 52–56, Apr. 1972.

A Technique for Computing Dispersion Characteristics of Shielded Microstrip Lines

TATSUO ITOH, SENIOR MEMBER, IEEE, AND RAJ MITTRA, FELLOW, IEEE

***Abstract*—The boundary value problem associated with the shielded microstrip-line structure is formulated in terms of a rigorous hybrid-mode representation. The resulting equations are subsequently transformed, via the application of Galerkin's method in the spectral domain, to yield a characteristic equation for the dispersion properties of shielded microstrip lines. Among the advantages of the method are its simplicity and rapid convergence. Numerical results are included for several different structural parameters. These are compared with other available data and with some experimental results.**

I. INTRODUCTION

With the increasing use of microstrip-line circuits at higher frequencies, a number of workers have studied the dispersion properties of microstrip lines [1]. Mittra and Itoh [2] used the singular integral equation approach for the shielded microstrip line, while Krage and Haddad [3] employed the Fourier-series expansion of the fields in the shielded microstrip line followed by a point-matching technique.

Manuscript received March 7, 1974; revised June 10, 1974. This work was supported in part by the National Science Foundation under Grant GK 36854, and in part by the U. S. Research Office under Grant DA-ARO-D-31-124-71-G77.

The authors are with the Department of Electrical Engineering, University of Illinois at Urbana-Champaign, Urbana, Ill. 61801.

Itoh and Mittra have recently demonstrated the application of a novel technique, called the spectral-domain analysis, to the problem of determining the dispersion characteristics of open microstrip lines [4]. In this short paper the technique just mentioned is extended to apply to the shielded microstrip-line problem. Some of the unique features of the method, which is based on the application of Galerkin's method in the finite Fourier transform domain, are as follows: a) the spectral method is numerically simpler and more efficient than the conventional space-domain techniques. This is due primarily to the fact that in the present method solutions are extracted from algebraic equations rather than from coupled integral equations typically appearing in the conventional space-domain approaches; b) the use of transforms allows one to convert convolutions into algebraic products, thus avoiding the necessity of numerical evaluation of complicated integrals, a process which is often extremely time consuming; c) typically, eigenvalues for the propagation constants are obtained from a determinantal equation, and the behavior of the field distribution of the eigenmodes are not readily discernible [2]. However, in the present method the physical nature of the field corresponding to each mode is directly incorporated in the process of solution via the appropriate choice of basis functions.

II. FORMULATION OF THE PROBLEM

Fig. 1 shows the cross section of the shielded microstrip line. The structure is assumed to be uniform and infinite in the z direction. The infinitely thin strip and the shield case are perfect conductors. It is also assumed that the substrate material is lossless and its relative permittivity and permeability are ϵ_r and μ_r, respectively.

The hybrid-field components in the microstrip line can be expressed in terms of a superposition of the TE and TM fields, which are in turn derivable from the scalar potentials $\psi^{(e)}$ and $\psi^{(h)}$. For instance

$$E_{zi} = j\,\frac{k_i^2 - \beta^2}{\beta}\,\psi_i^{(e)}(x,y)\,\exp(-j\beta z) \tag{1a}$$

$$H_{zi} = j\,\frac{k_i^2 - \beta^2}{\beta}\,\psi_i^{(h)}(x,y)\,\exp(-j\beta z) \tag{1b}$$

$$k_1 = \omega(\epsilon_r\mu_r\epsilon_0\mu_0)^{1/2}, \quad k_2 = \omega(\epsilon_0\mu_0)^{1/2} = k_0 \tag{2}$$

where β is the unknown propagation constant and ω is the frequency. The superscripts (e) and (h) are associated with the TM- and TE-type fields, respectively. The subscripts $i = 1,2$ serve to designate region 1 (substrate) or 2 (air). Other field components can be easily derived from Maxwell's equations.

From this point on, we proceed essentially in a manner similar to [4]. However, the bounded nature of the geometry of the shielded structure requires the use of the finite Fourier transform instead of the conventional Fourier transform over an infinite range. The

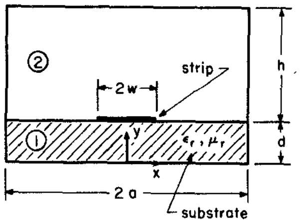

Fig. 1. Cross section of the shielded microstrip line.

Fourier transform[1] of the scalar potentials is defined via

$$\tilde{\psi}_i^{(p)}(n,y) = \int_{-a}^{a} \psi_i^{(p)}(x,y) \exp(j\hat{k}_n x)\, dx, \quad \begin{matrix} i = 1,2 \\ p = e \text{ or } h \end{matrix} \tag{3}$$

where $\hat{k}_n = (n - 1/2)\pi/a$ for E_z even–H_z odd modes and $\hat{k}_n = n\pi/a$ for E_z odd–H_z even modes ($n = 1,2,\cdots$).

The next step is to Fourier transform all the field components using expressions similar to (3) and apply the appropriate continuity and boundary conditions in the Fourier transform or spectral domain. After some mathematical manipulations this leads to

$$\tilde{G}_{11}(n,\beta)\tilde{J}_x(n) + \tilde{G}_{12}(n,\beta)\tilde{J}_z(n) = \tilde{E}_z(n) \tag{4a}$$

$$\tilde{G}_{21}(n,\beta)\tilde{J}_x(n) + \tilde{G}_{22}(n,\beta)\tilde{J}_z(n) = \tilde{E}_x(n) \tag{4b}$$

where

$$\tilde{G}_{11} = \tilde{G}_{22} = \hat{k}_n\beta(\gamma_2 \tanh \gamma_2 h + \mu_r\gamma_1 \tanh \gamma_1 d)/\det \tag{5a}$$

$$\tilde{G}_{12} = [(\epsilon_r\mu_r k_0^2 - \beta^2)\gamma_2 \tanh \gamma_2 h + \mu_r(k_0^2 - \beta^2)\gamma_1 \tanh \gamma_1 d]/\det \tag{5b}$$

$$\tilde{G}_{21} = [(\epsilon_r\mu_r k_0^2 - \hat{k}_n^2)\gamma_2 \tanh \gamma_2 h + \mu_r(k_0^2 - \hat{k}_n^2)\gamma_1 \tanh \gamma_1 d]/\det \tag{5c}$$

$$\det = (\gamma_1 \tanh \gamma_1 d + \epsilon_r\gamma_2 \tanh \gamma_2 h)(\gamma_1 \coth \gamma_1 d + \mu_r\gamma_2 \coth \gamma_2 h) \tag{5d}$$

and

$$\tilde{J}_x(n) = \int_{-w}^{w} J_x(x) \exp(j\hat{k}_n x)\, dx$$

$$\tilde{J}_z(n) = \int_{-w}^{w} J_z(x) \exp(j\hat{k}_n x)\, dx$$

are the transforms of strip currents J_x and J_z. Also

$$\tilde{E}_z(n) = K_z \int_{-a}^{a} E_z(x,d) \exp(j\hat{k}_n x)\, dx$$

$$\tilde{E}_x(n) = K_x \int_{-a}^{a} E_x(x,d) \exp(j\hat{k}_n x)\, dx$$

where K_z and K_x are some constants. Notice that $\tilde{E}_z$ and $\tilde{E}_x$ are unknown since the electric fields $E_z(x,d)$ and $E_x(x,d)$ are unknown for $w < |x| < a$, though they are zero on the strip. Also note that (4) is a set of two algebraic equations in contrast to the coupled integral equations appearing in the conventional space-domain analyses. As alluded to earlier, this is the principal advantage of the present method of formulation.

III. METHOD OF SOLUTION

In this section an efficient method for solving (4) is presented. It is first noted that the two equations in (4) contain four unknowns $\tilde{J}_x$, $\tilde{J}_z$, $\tilde{E}_x$, and $\tilde{E}_z$. However, by using certain properties of these functions, the two latter unknowns $\tilde{E}_x$ and $\tilde{E}_z$ can be eliminated from these equations. To this end, Galerkin's method is applied in the spectral domain for solving these equations. The first step is to expand unknown $\tilde{J}_x$ and $\tilde{J}_z$ in terms of known basis functions $\tilde{J}_{xm}$ and $\tilde{J}_{zm}$:

$$\tilde{J}_x(n) = \sum_{m=1}^{M} c_m \tilde{J}_{xm}(n) \tag{6a}$$

$$\tilde{J}_z(n) = \sum_{m=1}^{N} d_m \tilde{J}_{zm}(n) \tag{6b}$$

where c_m and d_m are unknown constants. The basis functions $\tilde{J}_{xm}$ and $\tilde{J}_{zm}$ must be chosen such that their inverse Fourier transforms are nonzero only on the strip $|x| < w$. After substituting (6) into (4), one takes inner products with the basis functions $\tilde{J}_{xi}$ and J_{zi} for different values of i. This process yields the matrix equation

$$\sum_{m=1}^{M} K_{im}^{(1,1)} c_m + \sum_{m=1}^{N} K_{im}^{(1,2)} d_m = 0, \qquad i = 1,2,\cdots,N \tag{7a}$$

$$\sum_{m=1}^{M} K_{im}^{(2,1)} c_m + \sum_{m=1}^{N} K_{im}^{(2,2)} dm = 0, \qquad i = 1,2,\cdots,M \tag{7b}$$

where from the definition of the inner product

$$K_{im}^{(1,1)}(\beta) = \sum_{n=1}^{\infty} \tilde{J}_{zi}(n)\tilde{G}_{11}(n,\beta)\tilde{J}_{xm}(n) \tag{8a}$$

$$K_{im}^{(1,2)}(\beta) = \sum_{n=1}^{\infty} \tilde{J}_{zi}(n)\tilde{G}_{12}(n,\beta)\tilde{J}_{zm}(n) \tag{8b}$$

$$K_{im}^{(2,1)}(\beta) = \sum_{n=1}^{\infty} \tilde{J}_{xi}(n)\tilde{G}_{21}(n,\beta)\tilde{J}_{xm}(n) \tag{8c}$$

$$K_{im}^{(2,2)}(\beta) = \sum_{n=1}^{\infty} \tilde{J}_{xi}(n)\tilde{G}_{22}(n,\beta)\tilde{J}_{zm}(n). \tag{8d}$$

One can prove the right-hand sides of (4) are eliminated via the use of Parseval's theorem, because the currents $J_{zi}(x)$, $J_{xi}(x)$ and the field components $E_z(x,d)$ $E_x(x,d)$ are nonzero in the complementary regions of x.

Now the simultaneous equations (7) are solved for the propagation constant β at each frequency ω by setting the determinant of the coefficient matrix equal to zero and by seeking the root of the resulting equation. The dispersion property of the microstrip line is derived from the obtained value of β.

Before ending this section it is pointed out that in the present method the solution can be systematically improved by increasing the size $(M + N)$ of the matrix.

IV. NUMERICAL COMPUTATION AND RESULTS

The choice of the basis functions is important for the numerical efficiency of the method [4]. If the first few basis functions approximate the actual unknown current reasonably well, the necessary size of the matrix can be held small for a given accuracy of the solution. For the dominant mode, the following forms have been chosen for J_{z1} and J_{x1}:

$$J_{z1}(x) = \begin{cases} \dfrac{1}{2w}\left[1 + \left|\dfrac{x}{w}\right|^3\right], & |x| < w \\ 0, & w < |x| < a \end{cases}$$

$$J_{x1}(x) = \begin{cases} \dfrac{1}{w}\sin\dfrac{\pi x}{w}, & |x| < w \\ 0, & w < |x| < a. \end{cases}$$

The Fourier transforms of the above current distributions are given by

$$\tilde{J}_{z1}(n) = \frac{2\sin(\hat{k}_n w)}{\hat{k}_n w} + \frac{3}{(\hat{k}_n w)^2}\left\{\cos(\hat{k}_n w) - \frac{2\sin(\hat{k}_n w)}{\hat{k}_n w} + \frac{2[1 - \cos(\hat{k}_n w)]}{(\hat{k}_n w)^2}\right\} \tag{9a}$$

$$\tilde{J}_{x1}(n) = \frac{2\pi \sin(\hat{k}_n w)}{(\hat{k}_n w)^2 - \pi^2}. \tag{9b}$$

[1] Henceforth, Fourier transform referred to in the rest of this paper will imply finite Fourier transform.

It is worthwhile mentioning here that the forms of J_{z1} and $\tilde{J}_{z1}$ are identical to those used by Denlinger [5].

A similar expression can be used for higher order $\tilde{J}_{zi}$ and $\tilde{J}_{xi}$. The dispersion relation has been calculated for two choices of matrix size: 1) $N = 1$, $M = 0$ and 2) $N = M = 1$. In the first case only the axial component J_{z1} of the step current is retained. This case may be called the zero-order approximation while choice 2) is the first-order approximation.

It should be noted that, although the computation of matrix elements given by (8) involves the evaluation of infinite summations, these summations can be efficiently evaluated, since for large n each term in the summations behaves as $(\hat{k}_n w)^{-3}$.

Fig. 2 shows the effective dielectric constant computed by the present method using matrix sizes 1) and 2). The definition of the effective dielectric constant is

$$\epsilon_{\text{eff}} = \left(\frac{\lambda}{\lambda_g}\right)^2 = \left(\frac{\beta}{k_0}\right)^2$$

where λ_g is the guide wavelength. The difference of the zero- and first-order approximation is relatively small. Some test calculations using a larger size matrix have shown that the difference from the first-order solution is so small that the results cannot be distinguished on the graphical figure.

Fig. 3 shows the ratio of guide wavelength to the free-space wavelength. Since the zero- and first-order curves are indistinguishable on this figure, only the first-order results are plotted. The present results are compared with the data in [2], and the agreement is quite good. Experimental results for an open microstrip line reported in [2] are also reproduced.

Typical computation time on the CDC G-20 computer (ten times slower than the IBM 360/75) was about 10–15 s/structure for the first-order approximation when the matrix elements were computed accurately to four digits or better.

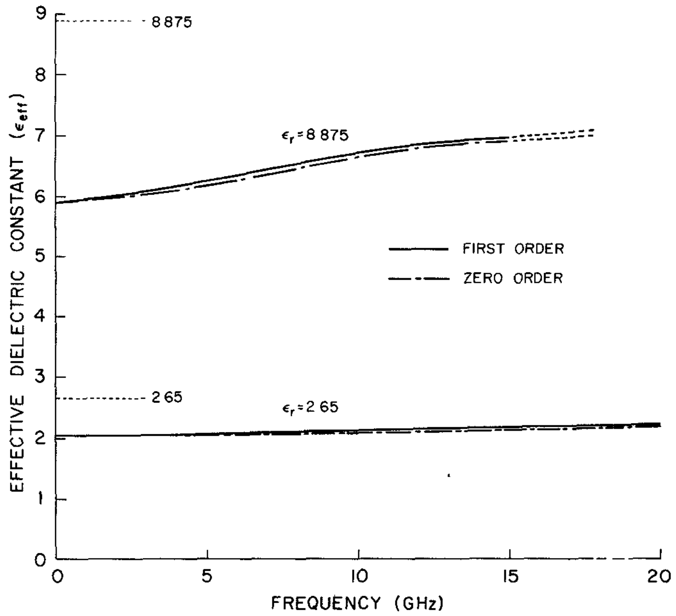

Fig. 2. Effective dielectric constant ϵ_{eff} versus frequency.

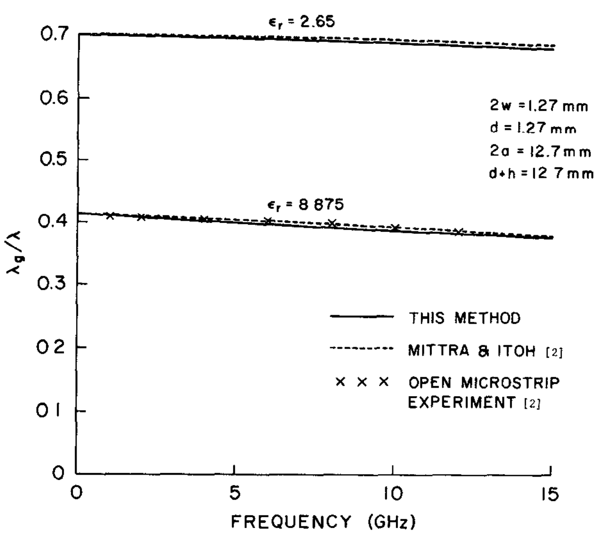

Fig. 3. Normalized guide wavelength λ_g/λ versus frequency.

V. CONCLUSION

An efficient numerical method has been presented for obtaining the dispersion properties of shielded microstrip lines. The method, which is based on Galerkin's method applied in the spectral domain, has a number of numerically attractive features. Numerical results obtained by the present method have been compared with other available data.

REFERENCES

[1] G. I. Zysman and D. Varon, "Wave propagation in microstrip transmission lines," presented at the Int. Microwave Symp., Dallas, Tex., May 1969, Session MAM-I-1.
[2] R. Mittra and T. Itoh, "A new technique for the analysis of the dispersion characteristics of microstrip lines," *IEEE Trans. Microwave Theory Tech.*, vol. MTT-19, pp. 47–56, Jan. 1971.
[3] M. K. Krage and G. I. Haddad, "Frequency-dependent characteristics of microstrip transmission lines," *IEEE Trans. Microwave Theory Tech.*, vol. MTT-20, pp. 678–688, Oct. 1972.
[4] T. Itoh and R. Mittra, "Spectral-domain approach for calculating the dispersion characteristics of microstrip lines," *IEEE Trans. Microwave Theory Tech.* (Short Papers), vol. MTT-21, pp. 496–499, July 1973.
[5] E. J. Denlinger, "A frequency dependent solution for microstrip transmission lines," *IEEE Trans. Microwave Theory Tech.*, vol. MTT-19, pp. 30–39, Jan. 1971.

Mixed Mode Filters

DAVID A. TAGGART AND ROBERT D. WANSELOW,
SENIOR MEMBER, IEEE

***Abstract*—Mixed mode bandpass filters are described which utilize alternating TE_{011}° and TE_{n11}° circular waveguide cavity modes. This novel filter configuration exhibits both excellent unloaded Q and spurious mode response characteristics. The use of mixed resonant modes makes possible the design of microwave filters for both in-line side wall connected cylindrical resonators as well as folded planar filter configurations, whereby cross-coupling between selected resonators can be realized.**

I. INTRODUCTION

It is well known that the design performance of narrow-band cylindrical TE_{011}° mode resonator filters exhibits a very low insertion loss response by virtue of the relatively high unloaded Q that this mode affords [1]. However, due to the relatively large cavity (diameter) size required to support the TE_{011}° mode, resonators operating in this mode tend to display unwanted spurious passband resonances. As described by Matthaei and Weller [2] these spurious resonances can be removed for all practical purposes via the trapped-mode concept. To a lesser degree these spurious modes may also be suppressed by employing alternate right-angle coupling between adjacent cylindrical cavity walls as indicated by [1, p. 923]. However, even though the unloaded Q of the trapped-mode TE_{011}° circular cavity resonator is somewhat higher than that available from conventional rectangular $TE_{101}^{\square}$ mode resonantors, it is still well below that realizable from conventional TE_{011}° mode cavity filters. In fact, the unloaded Q of the trapped-mode TE_{011}° resonator is also less than TE_{n11}° mode resonantors ($n > 1$) [2, p. 583]. An additional technique for the elimination of spurious modes is the utilization of a polyiron mode suppressor on the back side of the end wall tuning plunger [3]. Unfortunately, the unloaded Q of the TE_{011}° mode is reduced [1, p. 934] when employing dissipative material.

Manuscript received March 11, 1974; revised May 9, 1974.
The authors are with the TRW Systems Group, Redondo Beach, Calif. 90278.